Appl. Phys. B 90, 311–315 (2008)
DOI: 10.1007/s00340-007-2858-5

Applied Physics B
Lasers and Optics

W. CHEN[1,✉]
A.A. KOSTEREV[2]
F.K. TITTEL[2]
X. GAO[3]
W. ZHAO[3]

H_2S trace concentration measurements using off-axis integrated cavity output spectroscopy in the near-infrared

[1] Laboratoire de Physicochimie de l'Atmosphère, CNRS UMR 8101, Université du Littoral Côte d'Opale, 189A, Av. Maurice Schumann, 59140 Dunkerque, France
[2] Rice Quantum Institute, MS 366, Rice University, 6100 Main St., Houston, TX 77005, USA
[3] Anhui Institue of Optics and Fine Mechanics, Chinese Academy of Sciences, P.O. Box 1125, 350 Shushanhu Road, Hefei, Anhui 230031, P.R. China

Received: 17 October 2007
Published online: 7 December 2007 •

ABSTRACT Hydrogen sulfide (H_2S) trace detection has been performed by means of a DFB diode laser-based off-axis integrated cavity output spectroscopy (OA-ICOS) near 1571.6 nm. A minimum detectable concentration of 670 ppb (3σ) for a 2 s averaging time was obtained with an effective optical pathlength of ~ 1.8 km.

PACS 07.07.Df; 33.20.Ea; 42.62.Fi; 82.80.Gk

1 Introduction

Hydrogen sulfide (H_2S) is a colorless, toxic, flammable gas. Oil and gas fields, tankers, production facilities and industrial petroleum operations have the potential to emit significant amounts of H_2S. Other sources of H_2S include the holds of ships, mine shafts, paper pulp mills, swamps, and sewers. H_2S also occurs in volcanic gases and some well waters. Long-term, low-level exposure to concentrations below 150 ppb can cause olfactory fatigue, loss of appetite, headaches, irritability, poor memory, and dizziness. Exposure to hydrogen sulfide at levels up to 100 to 150 ppm can result in eye irritation, sore throat and cough, and shortness of breath. Concentrations of 700–800 ppm or higher can be fatal.

H_2S is one of the two most abundant volcanically emitted sulfur-bearing species. Monitoring of changes in the release of the principal components of volcanic gases (carbon dioxide and sulfur dioxide) from a volcano can be used to provide early warning of a volcanic eruption. However, when hydrothermal or meteoric water systems are present in the subsurface, an increase in SO_2 emissions may not be detected at the surface. In this case, monitoring of CO_2 and H_2S emission rates can be used as indicators for magmatic intrusions of the environment [1], because CO_2 and H_2S emissions are less soluble in water and emissions of these gaseous species should therefore increase. In addition, the SO_2/H_2S ratio can be used for the determination of the drying out of a hydrothermal or ground-water system in case of a magma intrusion.

✉ Fax: +33 3 28 65 82 44, E-mail: chen@univ-littoral.fr

There is a considerable interest in the instrumental development for in situ and realtime H_2S concentration measurements for various field applications. H_2S detection at ppm levels has been previously reported using diode laser-based wavelength modulation spectroscopy, two-tone frequency modulation technique and photoacoustic detection. An H_2S detection limit of < 10 ppm based on wavelength-modulation spectroscopy of a distributed feedback (DFB) laser operating at 1576 nm and harmonic detection was reported by Weldon et al. [2]. Two-tone frequency modulation spectroscopy was employed by Modugno et al. to investigate H_2S detection with a sensitivity of 4 ppm (using a 1-m absorption path length) for the 1577.32 nm component of the $\nu_1 + \nu_2 + \nu_3$ band [3]. In [4], Varga et al. reported a H_2S concentration measurement platform based on photoacoustic spectroscopy (PAS) with a minimum detectable H_2S concentration of 0.5 ppm (3σ). In this work, we demonstrate the feasibility of H_2S trace detection by means of off-axis integrated cavity output spectroscopy (OA-ICOS) using a DFB diode laser operating near $\lambda = 1571.6$ nm. A minimum detectable concentration of 670 ppb (for signal-to-noise ratio = 3) was obtained for a 2 s averaging time.

2 Selection and intensity study of absorption line

Spectral parameters of H_2S in the near infrared are not available in either the GEISA [5] or the HITRAN [6] spectroscopic database. Therefore, a FT-IR spectrum of H_2S (Fig. 1, bottom line) from the Pacific Northwest National Laboratory (PNNL) database, acquired at 1 atm pressure, was used for absorption line selection. In the spectral region of 6359–6366 cm^{-1}, accessible with the DFB diode laser available for this work, an absorption line at ~ 6362.87 cm^{-1} was selected for spectroscopic H_2S trace detection. The top line in Fig. 1 is a direct absorption data for a CO_2 reference cell in the same spectral region. The $R(20)$ CO_2 line of the $3\nu_1$ band at 6362.5038 cm^{-1} was used as the frequency reference as well as for determining the effective optical path length of the OA-ICOS cavity using a calibrated CO_2 concentration.

As certain line parameters (such as the line intensity and pressure broadening coefficients) of H_2S are not available in the spectroscopic database for the spectral region explored in

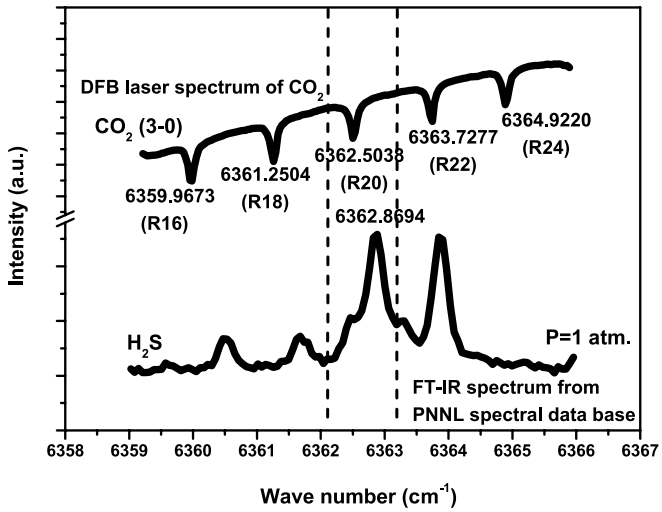

FIGURE 1 Absorption spectra of H_2S for spectral line selection: PNNL data (*bottom line*) in comparison with the observed CO_2 absorption (*top line*) in a reference cell using our DFB diode laser

the present work, spectroscopic studies were carried out on the line absorption intensity for the selected spectral line with direct absorption spectroscopy. This study was performed with a spectrometer based on a fiber-coupled telecom-grade external cavity diode laser (from Tunics Plus). The spectrometer was described in [7]. In brief, the laser source, emitting single-mode and single-frequency radiation with a maximum optical power of 5 mW, is continuously tunable in the near infrared from 1500 to 1640 nm (C and L bands) with a wavelength resolution of 0.001 nm ($\sim 4 \times 10^{-3}\,\mathrm{cm}^{-1}$). The laser emission linewidth, determined by heterodyne measurements is less than 1 MHz. The laser output power was split off into two components. The main part was coupled to a fiber pigtailed collimator using a GRIN (GRadient INdex) lens ($f = 4.7$ mm) which formed a collimated beam of 1 mm in diameter, and which was then directed to a Herriott multipass cell. This cell, equipped with a wedged entrance window, has a fixed optical path of 100-m and a volume of 3.2 L (New Focus, Model 5612). The gas pressure inside the cell was measured with a capacitance manometer (Barocel Model 1000 MB NW16) designed for the 0.1–1000-mbar range, with a resolution of 0.1 mbar and a 0.15% accuracy. The radiation exiting the cell was focused onto an InGaAs photodiode detector. The remaining laser emission was fiber-coupled to a wavemeter (Burleigh, Model WA-1500) for wavelength measurements with a resolution of 10^{-4} nm and a relative accuracy of about $\pm 10^{-7}$. An H_2S absorption spectrum acquired in the 1530–1640 nm region (6097.5–6535.9 cm^{-1}) is shown in Fig. 2. This high-resolution spectrum has been recorded with 3 mbar pure H_2S in a 100-m long multipass cell at room temperature.

The high-resolution Fourier transform infrared spectrum of H_2S was recently reported by Ulenikov et al. [8] and Liu et al. [9] for the region of the 5500 to 6650 cm^{-1} spectral region. Based on this study, the absorption feature selected in the present work was assigned to the $7_{1,6}$–$6_{1,5}$ (6362.87675 cm^{-1}) and $7_{2,6}$–$6_{2,5}$ (6362.87675 cm^{-1}) overlapping transitions of

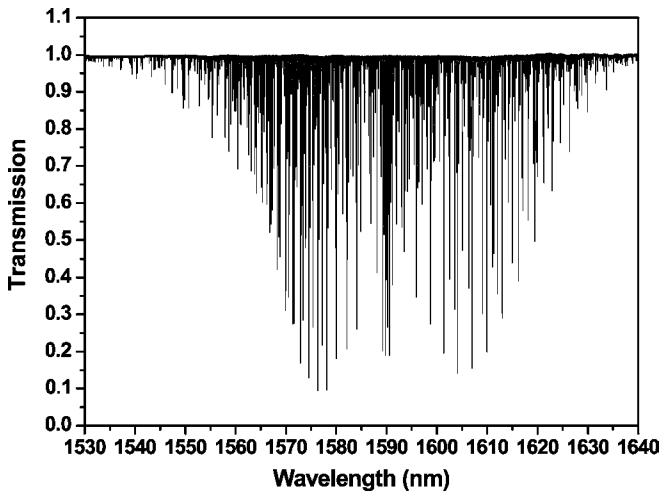

FIGURE 2 High-resolution direct absorption spectrum of H_2S in the near-infrared region of 1530–1640 nm (6097.5–6535.9 cm^{-1}) acquired using a widely tunable ECDL: 3 mbar pure H_2S in a 100-m long multipass cell at room temperature

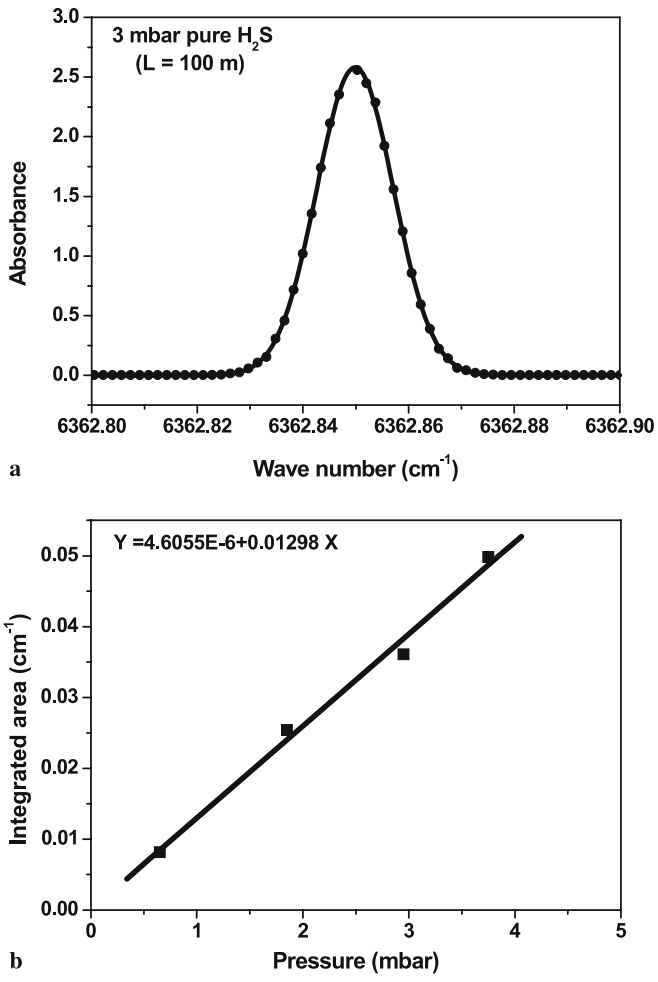

FIGURE 3 (**a**) Absorption spectrum fit of 3 mbar pure H_2S (*dots*) to a Voigt lineshape (*curve*); (**b**) Line intensity determination based on the linear fit of the integrated area under the absorption peak to the corresponding pure H_2S pressure. An effective line intensity value of $S_{\mathrm{eff}} = (5.25 \pm 0.35)10^{-23}$ cm/molecule was derived from the slope of the linear fit for the doublet line at 6362.87675 cm^{-1} resulting from the $7_{1,6}$–$6_{1,5}$ and $7_{2,6}$–$6_{2,5}$ overlapping transitions of the (111) band at 293.15 K

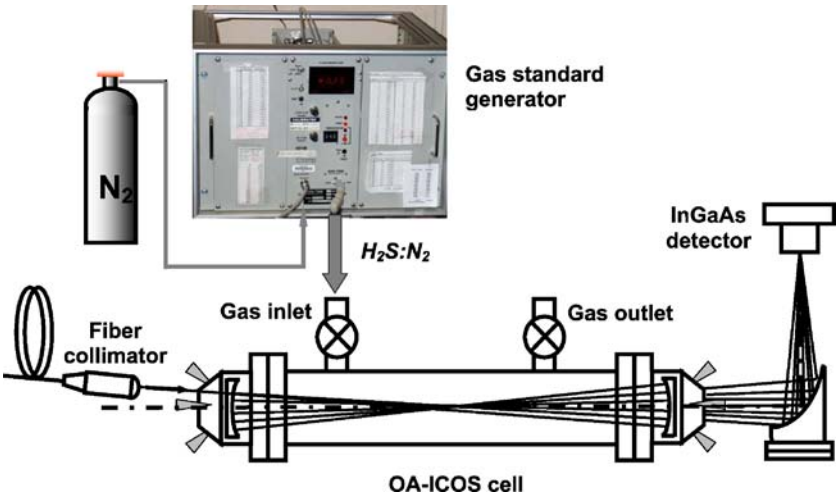

FIGURE 4 OA-ICOS experimental setup

the (111) band. The energy levels of the upper and lower rotational states are the same for this doublet.

Intensities of the $7_{1,6}$–$6_{1,5}$ and $7_{2,6}$–$6_{2,5}$ transitions of the (111) band at 6362.87675 cm^{-1} were investigated with direct absorption spectroscopy. The H_2S sample was purchased from Aldrich with a stated purity of 99.5%. Pure H_2S was introduced into the 100-m path length cell at a temperature of $T = 293.15$ K and at four pressures P: 0.65, 1.85, 2.95, and 3.75 mbar. The direct absorption spectrum of H_2S was measured for each pressure and fitted to a Voigt lineshape to determine the integrated area, A_I (in [cm^{-1}]), enclosed by the spectral line. Figure 3a shows a fitted absorption spectrum (dots) of 3 mbar pure H_2S using a Voigt lineshape model (curve). The integrated absorbance was plotted as a function of pressure. The line intensity of the selected line was retrieved from the slope of the linear fit of the integrated area to the pressure (Fig. 3b) by using the following expression with the help of a validated H_2S calibration standard:

$$S = \frac{A_I}{P} \times \frac{P_0 T}{N_L T_0 L C_{ppm}} \times 10^6 , \quad (1)$$

where S is the molecular absorption line intensity in [$cm^{-1}/(molecule\,cm^{-2})$], $N_L = 2.6868 \times 10^{19}$ molecules/cm^3, is the Loschmidt number at $T_0 = 273.15$ K and $P_0 =$ 760 Torr, L is the optical absorption path length in [cm].

An effective line intensity value of $S_{eff} = (5.25 \pm 0.35)$ 10^{-23} cm/molecule was found for the doublet line at 6362.87675 cm^{-1} resulting from the $7_{1,6}$–$6_{1,5}$ and $7_{2,6}$–$6_{2,5}$ overlapping transitions of the (111) band at 293.15 K.

3 OA-ICOS experimental setup

The OA-ICOS approach is based on the use of a high finesse optical cavity to achieve a long effective optical path length, often reaching several kilometers [10–12]. The experimental setup employed in the present work is depicted in Fig. 4. The OA-ICOS cavity consisted of two 1″ diameter spherical mirrors (1 m radius of curvature) separated by a 0.5-m long quartz coated stainless steel tube. The mirrors reflectivity was ∼ 99.995% at 1560 nm as specified by the manufacturer (Los Gatos Research), which corresponds to an

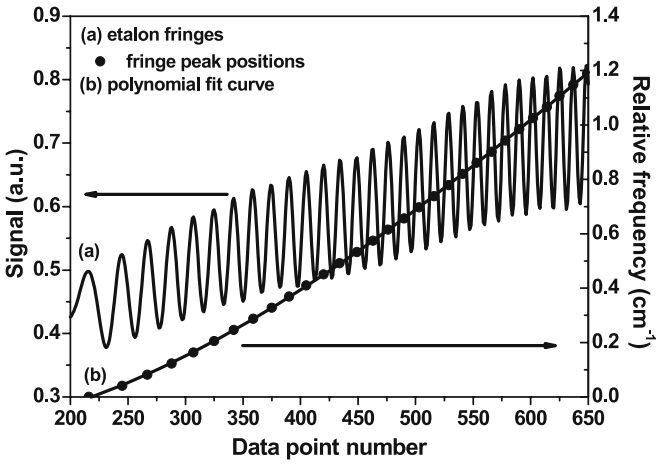

FIGURE 5 Curve (a): transmission fringes from an etalon used for frequency calibration. Curve (b): polynomial fit (*curve*) to the fringe peak positions (*dots*), used to calibrate the laser frequency relative to the number of the acquired data point

effective optical path length of ∼ 10 km in a 0.5-m long cavity with on-axis alignment. Three alignment screws located at one of the two cavity mirror mounts are piezo actuator-driven, which allows cavity length modulation. The diode laser source was a GaInAsP DFB laser diode (JDS Uniphase) operating in the near infrared at ∼ 1571.8 nm (∼ 6362 cm^{-1}). The single-mode diode laser was fiber pigtailed and delivered an output power of up to 63 mW. Frequency turning of the diode laser can be carried out by scanning either temperature (over 10 cm^{-1} with a tuning ratio of ∼ 0.4 cm^{-1}/K) or the current (over more than 1 cm^{-1}). An amplified, switchable-gain InGaAs detector (PDA10CS, Thorlabs) with the gain set to 70 dB and a bandwidth of 12 kHz was used for detection of the radiation exiting the optical cavity. Data acquisition of the absorption signal was performed using a National Instruments data acquisition card (DAQ card, Model 6062E) with a sampling rate of up to 500 kS/s.

4 H_2S trace concentration measurements

A gas standard generator (KIN-TEK Model 491 M) was used to provide a traceable calibration standard of H_2S.

The H_2S concentrations varied from 24 to 2.4 ppm in a diluting gas (nitrogen), determined by the gas flow rate.

The absolute DFB laser frequency was determined with the help of the HITRAN2004 database [6] by measuring simultaneously the direct absorption spectra of CO_2 and CO in reference cells while temperature tuning the diode. For H_2S trace detection only current tuning was used to scan laser wavelength over a spectral range of ~ 0.3 nm ($\sim 1.27\,cm^{-1}$) at a fixed laser temperature of 15.12 °C. As the wavelength scan by current tuning is usually nonlinear, transmission fringes from an etalon with a free spectral range of $0.041\,cm^{-1}$ were recorded (Fig. 5a) and used in combination with the measured reference spectra of CO_2 and CO for frequency metrology and calibration. Figure 5b shows a third-order polynomial fit (curve) to the fringe peak positions (dots), which was used to calibrate the laser frequency.

The OA-ICOS cell pressure was maintained at 100 Torr with a pressure controller (MKS Instruments type 649). The OA-ICOS cavity transmission spectra of H_2S were collected over $\sim 1\,cm^{-1}$ at $\sim 6362.8\,cm^{-1}$ by applying a voltage ramp to the DFB laser current driver at 10 Hz while maintaining the laser temperature constant. In order to improve the signal-to-noise ratio (SNR), 1000 cavity-enhanced transmission spectra were typically averaged for each H_2S concentration measurement.

In Fig. 6, we show the data processing of an OA-ICOS spectrum of 2.4 ppm H_2S: (a) The transmission data from the OA-ICOS cavity (A) and the background signal (B) in the absence of laser beam, used to determine the detector voltage offsets. (b) The OA-ICOS cavity transmission signal (curve) after background correction for the laser intensity ramp and a polynomial baseline simulation (dash). (c) The resulting absorption spectrum of 2.4 ppm H_2S together with a Voigt fit.

In order to check the linearity of the OA-ICOS based quantification of H_2S concentration, absorption spectra have been measured for different H_2S concentrations. In Fig. 7 the integrated absorbance, corresponding to the area under the absorption peak, is plotted versus the generated H_2S concentration. The plot confirms the expected linear dependence of the integrated OA-ICOS signal on the H_2S concentration.

Based on the experimentally estimated SNR of the spectral signal shown in Fig. 6c, a minimum detectable concentration of 670 ppb (for SNR = 3) was found for a 2 s averaging time. The detection sensitivity was limited by the interference fringe-like optical noise in the OA-ICOS cavity.

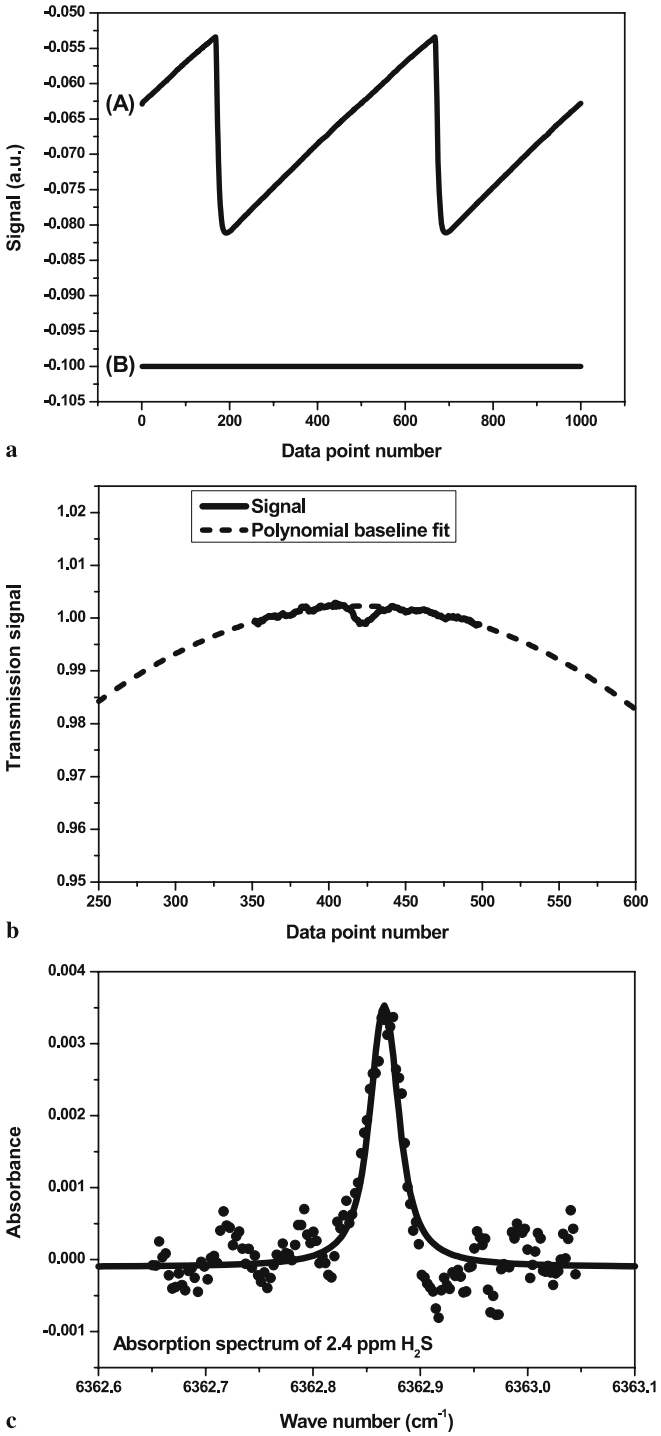

FIGURE 6 (**a**) The OA-ICOS cavity transmission signal (A) and the background signal (B) when blocking the laser emission. (**b**) OA-ICOS cavity transmission signal (*curve*) after background correction for laser intensity ramp and a polynomial-based baseline simulation (*dash*). (**c**) Absorption spectrum of 2.4 ppm H_2S (*dots*) along with a Voigt fit (*curve*). Based on the experimentally estimated SNR of the spectral signal, the corresponding minimum detectable concentration (MDC) was found to be 670 ppb (SNR = 3)

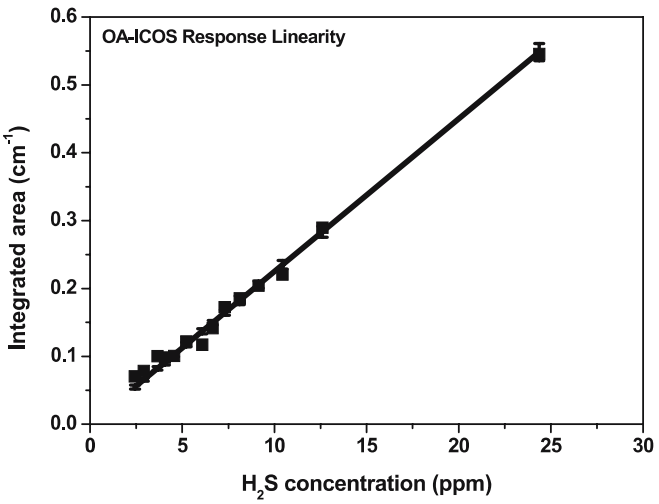

FIGURE 7 Linear dependence of the integrated OA-ICOS signal on the H_2S concentration

For the purpose of determining the effective optical path length realized with the OA-ICOS approach, a calibrated mixture of CO_2 in N_2 with a specified mixing ratio of 1% was used. An OA-ICOS transmission spectrum of the $R(20)$ CO_2 line of the $3\nu_1$ band at 6362.5038 cm^{-1} was recorded under the same experimental condition. On the basis of integrated absorbance, determined by least-squares fitting a Voigt lineshape to the experimental absorption spectrum, an effective path length of the OA-ICOS cavity of 1.81 km was retrieved. A detection sensitivity of $\sim 1.6 \times 10^{-10}$ cm^{-1} was determined based on an experimentally established minimum detectable fractional absorption of $\sim 3 \times 10^{-5}$.

5 Conclusion

In this work, we demonstrated the potential of trace detection of hydrogen sulfide by OA-ICOS using a DFB telecommunication laser operating at 1571.6 nm with a minimum detectable concentration of 670 ppb (SNR = 3).

For further improvement in detection sensitivity, the major challenge is to remove the fringe-like optical noise resulting from optical interference in the cavity. A wavelength modulation technique can be used in combination with OA-ICOS approach [13–16]. Wavelength modulation can effectively smooth out interference fringes in the cavity transmission spectrum [15, 16]. The additional advantage is the suppression of the $1/f$ laser and detector excess noise and baseline slope by use of second harmonic detection technique of wavelength modulation spectroscopy.

ACKNOWLEDGEMENTS This work is supported in part by the French regional program IRENI. W. Chen, X. Gao and W. Zhao acknowledge the financial support from the French International Program of Scientific Cooperation (CNRS/PICS No 3359). The authors acknowledge A. Liu and S. Hu (University of Science and Technology of China) for helpful discussions on H_2S spectra.

REFERENCES

1 R.B. Symonds, T.M. Gerlach, M.H. Reed, J. Volcanol. Geotherm. Res. **108**, 303 (2001)
2 V. Weldon, J. O'Gorman, P. Phelan, J. Hegarty, T. Tanbun-Ek, Sens. Actuators **B29**, 101 (1995)
3 G. Modugno, C. Corsi, M. Gabrysch, M. Inguscio, Opt. Commun. **145**, 76 (1998)
4 A. Varga, Z. Bozoki, M. Szakall, G. Szabo, Appl. Phys. B **85**, 315 (2006)
5 N. Jacquinet-Husson, N.A. Scott, A. Chédin, K. Garceran, R. Armante, A.A. Chursin, A. Barbe, M. Birk, L.R. Brown, C. Camy-Peyret, C. Claveau, C. Clerbaux, P.F. Coheur, V. Dana, L. Daumont, M.R. Debacker-Barilly, J.M. Flaud, A. Goldman, A. Hamdouni, M. Hess, D. Jacquemart, P. Köpke, J.Y. Mandin, S. Massie, S. Mikhailenko, V. Nemtchinov, A. Nikitin, D. Newnham, A. Perrin, V.I. Perevalov, L. Régalia-Jarlot, A. Rublev, F. Schreier, I. Schult, K.M. Smith, S.A. Tashkun, J.L. Teffo, R.A. Toth, Vl.G. Tyuterev, J. Vander Auwera, P. Varanasi, G. Wagner, J. Quant. Spectrosc. Radiat. Transf. **95**, 429 (2005)
6 L.S. Rothman, D. Jacquemart, A. Barbe, D. Chris Benner, M. Birk, L.R. Brown, M.R. Carleer, C. Chackerian Jr., K. Chance, L.H. Coudert, V. Dana, V.M. Devi, J.-M. Flaud, R.R. Gamache, A. Goldman, J.-M. Hartmann, K.W. Jucks, A.G. Maki, J.-Y. Mandin, S.T. Massie, J. Orphal, A. Perrin, C.P. Rinsland, M.A.H. Smith, J. Tennyson, R.N. Tolchenov, R.A. Toth, J. Vander Auwera, P. Varanasi, G. Wagner, J. Quant. Spectrosc. Radiat. Transf. **96**, 139 (2005)
7 J. Cousin, W. Chen, M. Fourmentin, E. Fertein, D. Boucher, F. Cazier, H. Nouali, D. Dewaele, M. Douay, L.S. Rothmann, J. Quantum Spectrosc. Radiat. Transf. **109**, 151 (2008)
8 O.N. Ulenikov, A.-W. Liu, E.S. Bekhtereva, O.V. Gromova, L.-Y. Hao, S.-M. Hu, J. Mol. Spectrosc. **234**, 270 (2005)
9 A.W. Liu, O.N. Ulenikov, G.A. Onopenko, O.V. Gromova, E.S. Bekhtereva, L. Wan, L.Y. Hao, S.-M. Hu, J.-M. Flaud, J. Mol. Spectrosc. **238**, 11 (2006)
10 J. Paul, L. Lapson, J. Anderson, Appl. Opt. **40**, 4904 (2001)
11 D. Baer, J. Paul, M. Gupta, A. O'Keefe, Appl. Phys. B **75**, 261 (2002)
12 Y. Bakhirkin, A. Kosterev, C. Roller, R. Curl, F. Tittel, Appl. Opt. **43**, 2257 (2004)
13 Y. Bakhirkin, A. Kosterev, R. Curl, F. Tittel, D. Yarekha, M. Giovannini, J. Faist, Appl. Phys. B **82**, 149 (2006)
14 W. Zhao, X. Gao, W. Chen, W. Zhang, T. Huang, T. Wu, H. Cha, Appl. Phys. B **86**, 353 (2007)
15 R. Vasudev, Appl. Phys. B **87**, 163 (2007)
16 R. Vasudev, Appl. Spectrosc. **60**, 926 (2006)